Modelling of adsorption/photodegradation phenomena on AC-TiO2 composite catalysts for water treatment detoxification

C. Telegang Chekem, V. Goetz, Y. Richardson, Gaël Plantard, J. Blin

Modelling of Adsorption/photodegradation phenomena on AC-TiO_2 composite catalysts for water treatment detoxification

C. Telegang Chekem[(1)(2)],V. Goetz[(1)], Y. Richardson[(2)],G. Plantard[(1)], J. Blin[(3)],

[(1)] PROMES- CNRS UPR 8521, PROcess Material and Solar Energy, Rambla de la Thermodynamique 66100 Perpignan, France

[(2)]Institut International d'Ingénierie de l'Eau et de l'Environnement (2iE), Laboratoire Energies Renouvelables et Efficacité Energétique, Rue de la Science, 01 BP 594, Ouagadougou 01, Burkina Faso

[(3)]Center of International Cooperation and Agronomic Research for Development (CIRAD), UPR Biomass, TA B-42/16, 73 rue Jean-François Breton, 34398 Montpellier Cedex 5, France

Abstract

1. Introduction

Adsorption on activated carbon (AC) is probably the most widespread separation unit operation industrially used to remove pollutants from water [1][2]. However, the energy cost of thermal regeneration remains a serious constraint for industries. Today, association of AC with TiO_2 appears as a promising way of getting a material with self-regeneration properties. Indeed, based upon TiO_2 photocatalysis activity [3], AC-TiO_2 composite materials could both adsorb and degrade the pollutant through photocatalyzed driven reactions [4]. Besides the self-regeneration capacity of AC-TiO_2 composite materials, they are also attractive regarding the multifunctionality and then process intensification resulting from the association of adsorption with photocatalysis [5].

A number of works addressed the experimental demonstration of the synergistic adsorption/photodegradation effects of AC-TiO_2 materials towards water detoxification [6–9]. However, the need still arises to get into a better understanding on how both phenomena really interact together and participate to the performance of the composite catalyst [10,11]. This requires the most convenient modelling of the hybrid process occurring in the complex system made up of the composite material and the polluted water. A good knowledge on how the composite material operates could provide various options for designing efficient water detoxification processes [4].

In their attempt in modelling AC-TiO_2 multifunctionality, a number of studies [12–14] use Langmuir-Hinshelwood (L-H) derived first order kinetic model, with the assumption that there exist somehow an equilibrium of the pollutant in liquid and adsorbed phases. Thus in such a configuration, mass transfer limitation associated to the pollutant sorption is neglected and it is assumed that the pollutant is almost instantly adsorbed to reach an equilibrium point according to a K distribution constant. However, given the high adsorption capacity and the high porosity of AC-TiO_2 composite materials, relevant adsorption transfer limitations are likely to affect the overall decontamination process, and therefore should also be integrated in a representative kinetic model.

In a previous paper of our research team, the modelling of hybrid processes involving adsorption and photodegradation was investigated on a system that consisted in a close fluid loop with an adsorption AC column separated from a TiO_2 supported catalytic media set in series [15]. The consistency between experimental and calculated data suggested its applicability for modelling the synergistic adsorption/photocatalysis phenomena. Regarding AC-TiO_2 composite materials, they offer the opportunity to get adsorption and photocatalytic unit operations running in a single reactor. The modelling of such a system must properly take into account the dual functionality of AC-TiO_2 materials, i.e. to set bridging calculations between adsorption and photodegradation mechanisms.

This paper investigates on a new simple formalism for mathematical modelling of pollutant removal from contaminated water, driven by the adsorption/photocatalysis hybrid process with AC-TiO_2 composite materials. The AC-TiO_2 materials prepared by a straightforward titania coating route of a homemade microporous AC, are tested to remove phenol from polluted water solution on lab scale batch experiments. The self-regeneration capacity of the composite catalysts has already been demonstrated experimentally, and addressed in a previous paper [16]. Here, the modelling of their adsorption/photodegradation dual functionality is carried out based upon the mass balance applied to the pollutant both in the liquid and adsorbed phases. The model is used for simulating the pollutant concentration profile in the treated solutions and on the composite material as well.

2. Materials and Methods

2.1. Preparation and characterization of AC-TiO_2 materials

A homemade AC was beforehand obtained from chemical activation (1M KOH) and pyrolysis (800 °C) of shea nut shells (SNS), a by-product from hand craft production units of shea butter in Burkina Faso. AC-TiO_2 catalyst has been obtained after reacting AC with a commercial TiO_2 sol (nanoparticles suspensions). The solid phase recovered after filtration was annealed at 250 °C on air and then 500 °C in Ar inert gas. N_2 adsorption desorption, scanning electron microscopy (SEM), energy dispersive spectroscopy (EDS) and X ray diffraction spectroscopy (XRD) have been used to determine the microstructural and textural properties of the resulting AC-TiO_2 composites. The reader could find more details on preparation and characterization of the catalysts in a previous paper of our research group [15].

2.2. Water detoxification experiments

Adsorption and photodegradation experiments were carried out in magnetically stirred beakers containing 100 mL of spiked phenol water solutions and small amounts of catalysts. A number of catalysts (*CATx*) with different titania contents ("*x*") were used. Photodegradation experiments were carried out under UV lamp (VL-320 model) delivering UV intensity within the range of solar UV light (≈ 24 W/m^2). The residual phenol concentration was determined with a double beam UV spectrophotometer at 270 nm wavelength.

Phenol adsorption isotherms were determined with the adsorption equilibrium data obtained by varying the AC-TiO_2 catalyst concentration within the range 0.1 – 8 g/L, while keeping constant the initial phenol concentration.

2.3. Modelling of adsorption/photodagradation coupled phenomena

2.3.1. Theoretical background

Photodegradation mechanisms through photo driven generation of excitons (holes and electrons) have already been addressed by a number of research studies. The mechanistic chain degradation through excitons transfer, either for production of highly reactive radical species, or straight towards the target molecules is well documented [17,18]. This clearly stands beyond the scope of this paper. Nevertheless, as far as AC-TiO_2 composites are concerned, the aforementioned degradations mechanisms globally depend on two main factor.

The first factor is the quantity of pollutant adsorbed on the catalyst if assumed that degradation only takes place on the adsorbed phase. This has to do with a kind of distribution coefficient (k) of the pollutant between solid and bulk liquid phases, with respect to transfer and diffusion mechanisms over both phases. Homogeneous Surface Diffusion Model (HSDM), Pore diffusion Model (PDM) and Pore Surface Diffusion Model (PSDM) can be used for modelling kinetics of absorptive species between and within different phases [19], with some adaptations for specific experimental conditions. The type and energy needed for adsorption is also well studied [17,20]. As a matter of fact, transfer of adsorptive species on a catalyst can then be represented by a versatile range of equations.

Secondly, the pollutant degradation is related to the capacity of the catalyst to use available UV light intensity to drive the photodegradation of the pollutant. This quantum yield will rely on the availability of the light over the reactor volume. Indeed, light distribution over the treated volume depends on optical properties of the system.

This point defines clearly another field of research and is the subject of many developments specifically devoted to an accurate knowledge of the irradiation profiles [21–23].

2.3.2. New model formalism

As far as water detoxification with AC-TiO_2 composites is concerned, little attention has been paid to interaction between adsorption and photodegradation, both phenomena taking place in the heterogeneous system made up of the porous composite material and the treated solution.

Despite the complexity of different phenomena involved, pollutant adsorption on an adsorbent porous grain can be expressed upon the Linear Driving Force (LDF) model. The model was used for the first time by Gleuckauf and Coates in 1947 and has been proven to describe successfully the wide range of phenomena involved [24]. LDF model is a Fick law-like model, represented in a simple but consistent way to describe complex systems. Interestingly, it considers that pollutant flux is driven by the gradient between the quantity of pollutant adsorbed at a given time q_t (mg.g^{-1}) and the quantity q_e (mg.g^{-1}) that would be at the equilibrium with the solution concentration. An equivalent mass transfer coefficient which can also be considered as an adsorption kinetic coefficient k_{ads} (s-1) is then included on the expression of the pollutant density flux N_f (mg.s^{-1}.g^{-1}), according to ***Eq. 1***.

$$N_f = k_{ads}(q_e - q_t) \tag{1}$$

k_{ads} can be expressed in several ways, depending on the shape and the size of the adsorbent porous grains. But typically, it also expresses the intraparticles mass transfer limitations [24] i.e before the pollutant reaches the TiO_2-NPs photodegradation sites on the catalyst.

On the other hand, under UV irradiation, the intrinsic degradation reaction rate (r in mg.g^{-1}.s^{-1}) on the catalyst is suggested to follow the first order kinetic law according to ***Eq.2***.

$$r = k_r.q_t \tag{2}$$

$$k_r = \alpha.\left(\frac{S}{V}\cdot I_{UV}\right) \tag{3}$$

According to ***Eq. 3,*** the degradation rate constant k_r (s^{-1}) depends on the production level of excitons (electrons and holes) and hydroxyl radicals $OH^{\cdot}$, assumed to be directly proportional to UV irradiation with respect to a kinetic parameter α (m^2.J^{-1}). It is also suggested that k_r depends on a volumetric level of irradiation, which is a function of UV irradiation I_{UV} (W.m^{-2}) at the surface S (m^2) of the reactor of volume V (m^3). This formalism is clearly a rough simplification and can fairly be applied for comparison of experiments performed on particles suspension with similar or close optical properties and same optical thickness.

Although there is still some debates on whether attacks of pollutant by radicals species take place in the bulk liquid phase or within the adsorbed phase, the last option is commonly accepted [25], especially with highly adsorbing materials like AC-TiO_2 catalysts. Taking into account the global heterogeneous system and the pollutant transfer over different phases and then its photodegradation onto the catalyst, the mass balances yield the differential equations ***Eq. 4*** and ***5***:

$$\frac{dC_t}{dt} = -k_{ads}.C_{cat}.(q_e - q_t) \tag{4}$$

$$\frac{dq_t}{dt} = k_{ads}.(q_e - q_t) - \alpha(\frac{S}{V}).I_{UV}.q_t \quad (5)$$

In both equations, the value of q_e is instantaneously obtained using the concentration of the pollutant C_t (mg.L^{-1}) and the catalyst dosage C_{cat} (g.L^{-1}) in the treated solution, according to adsorption isotherms expressions. This modelling formalism was previously used successfully by our research group on a different configuration system [15], and now used for the first time on AC-TiO_2 composite catalysts.

3. Results and discussion

3.1. Textural and structural properties of AC-TiO_2 catalysts

After TiO_2 coating on AC, the macropores surfaces were regularly covered by a layer of nanoparticles (NPs), despite the presence of few aggregates (***Fig. 1***). TiO_2 chemical nature of the deposition is evinced by the high titania content depicted on EDX spectrum and the XRD anatase profile, presented elsewhere [9][15].

Fig. 1.

It is worth mentioning that micropores are very useful towards adsorption of pollutant species like phenol [26]. ***Table 1*** shows that their volume represents the main part of total pores volume, as typically observed on commercial AC. The presence of micropores is consistent with the high surface areas developed on both AC and the catalyst obtained after TiO_2 coating. Actually, internal pore volume is not significantly affected by TiO_2-NPs which preferentially locate at the external macroporosity (***Fig 2.A***), unlike the degradation of pores volumes highlighted in the literature [4,13,14]. This suggests that the utilization of preformed NP_S sol used in this study prevents TiO_2 to enter and spoil AC internal micropores and surface areas, otherwise useful for pollutants adsorption.

Fig. 2.

3.2. Adsorption isotherms.

Phenol adsorption isotherms of catalysts of different titania content is presented in ***Fig. 3***. The upper position of the composite catalysts *CAT25* and *CAT14* as compared to uncoated AC isotherm suggests the higher adsorption capacity of the composite material, which is consistent with the increase of surface area (***Section 3.1***).

Fig. 3.

Considering isotherm profile, a consistent fitting is obtained with Langmuir model (***Table 1***). This could indicates that there exist a significant homogeneity on the adsorption surfaces, as far as adsorption centers are concerned [27]. However, it is almost accepted that different types of adsorption schemes intervene when organic pollutants are adsorbed on activated carbon. Adsorption can be physical, chemical, electrostatic or non-electrostatic, depending on surface chemistry of the catalyst, which is beyond the scope of this paper.

Table 1.

All the catalysts depicted the same typical adsorption and photodegradation kinetic profiles, obtained respectively with and then without UV light irradiation (***Fig. 4***). Without UV light, the kinetic curve drops rapidly and then stabilizes (at from 10 to 30 % of the initial concentration), indicating the adsorption equilibrium between bulk treated solution and the catalysts. The catalysts are saturated and no more able to remove the pollutant from the solution. Under UV light irradiation, the kinetic curve follows a similar first phase profile i.e a sharp drop within the first hour. However, the UV light free second stabilization phase is no longer observed, replaced by a gradual decrease of phenol concentration until almost total removal in the treated water.

Preliminary blank experiments (without the catalyst) showed that very few amount of phenol (< 2.5 %) is photolysed under UV light irradiation (result not shown, published elsewhere [16]). The same profile were observed when using neat titania without UV light, suggesting the negligible adsorption capacity of titania. It is with irradiated TiO_2 that the pollutant removal is driven by photodegradation.

3.3. Comparison between experiments and modelling data of phenol adsorption and photocatalytic degradation

When solving the set of differential ***Eq. 4*** and ***5***, K_{ads} and $\boldsymbol{\alpha}$ appear as characteristic parameters, describing the global kinetics of pollutant removal from the treated solution. The values of these two parameters were optimized using a MATLAB® code, which minimizes a criterion (***Eq. 6***) that compares the calculated concentration profiles C_{cal} (mg.L^{-1}) against the results obtained from experiments C_{exp} (mg.L^{-1}).

$$CRIT = \min\left[\frac{1}{n_{\exp}}\sum_{1}^{n_{\exp}}\sqrt{\left(\frac{C_{\exp}-C_{calc}}{C_{\exp}}\right)^2}\right] \qquad (6)$$

Numerical integration of ***Eq. 4*** and ***5*** is carried out with the following starting conditions: $t_0 = 0$, $q_o = 0$, $C_o = 100$ mg.L^{-1}. n_{exp} is the total number of experimental points made up of sets of data obtained under different experimental conditions (catalysts of different titania content and experiments with and/or without UV light).

3.3.1. First run of phenol removal.

Fig. 4. sets out with the comparison between experimental and simulated concentrations of the pollutant in the treated solution, obtained with catalysts of different titania contents. It is worth mentioning that the same values of kinetic parameters (K_{ads}= 9.02 x 10^{-4} s^{-1} and α= 100.5 x 10^{-6}.m^3.J^{-1}) were always applicable.

Fig. 4

One can observe that simulations fit fairly well the experimental profiles, regardless the experiment conducted with or without UV, indicating the consistency of the model hypothesis. According to ***Eq. 4*** and ***5***, a photodegradation coefficient k_r can be obtained knowing the value of the parameter $\boldsymbol{\alpha}$. Under the experimental conditions observed in this study (reactor shape and UV irradiation), k_r has been calculated (***Eq.6***). Besides these two kinetic coefficients, adsorption on the catalyst is driven by q_e-q_t gradient while photodegradation basically increases with the amount of pollutant adsorbed on the material. Adsorption kinetic coefficient (k_{ads}= 9.02 x 10^{-4} s^{-1}) is virtually a hundred time higher than k_r (7.035 x 10^{-6} s^{-1}). This indicates why no significant difference is observed between kinetic profiles under or without UV irradiation, within the first hour of high adsorption activity. During this phase, degradation activity is negligible as compared to adsorption. However, when adsorption phenomena are about to stabilize (after an hour under UV), photodegradation contribution can be actually perceived on pollutant removal profile. In fact, at that moment, the concentration gradient q_e-q_t (which drives transfer over different phases) is significantly decreased, together with adsorption phenomena, despite the high adsorption kinetic coefficients. On the contrary at the same moment, photodegradation activity is reinforced by the higher amount of pollutant on the catalyst (q_t), despite the relative low value of k_r (***Fig. 5***).

Fig. 5

When the system is not UV irradiated ($I_{UV} = 0$), degradation activity is negligible and this is consistent with the stabilization of the pollutant concentration within the first hour of treatment.

One can also observe a consistency between the simulated and experimental data when different initial concentrations of the pollutant (200, 150, 100 and 50 mg.L^{-1}) are used (***Fig. 4.d***). Interestingly, this suggests that the model can be applied in real treatment plants where variation of pollutant input concentrations in the treated water can be registered.

3.3.2. Successive utilization of catalyst

Simulation of the pollutant concentration over several runs corresponding to catalyst reuses was carried out. For mathematical simulation, the relation between initial values t_0 and C_o from run "*n*" to run "*n+1*" is given by ***Eq. 7*** and ***8***. The profile of the amount of pollutant on the adsorbed phase also arises from simulations, using the initial conditions applied to ***Eq.9***.

$$t_o(n+1) = t_f.(n) \tag{7}$$

$$C_O(n+1) = C_0(n) \tag{8}$$

$$q_o(n+1) = q_f(n) \tag{9}$$

q_f (mg.L^{-1}) being the simulated adsorption capacity at the end of a given run.

Simulated profiles fit fairly well the experimental data and suggest the applicability of the model for materials reuse. This entails the fact that the model describes well the efficiency of the composite material which gradually decreases along with the number of runs. Interestingly, the model can also depict the amount of pollutant in the absorbed phase (***Fig. 6***), hardly obtained experimentally under UV light anyway. The results clearly demonstrate how the amount of pollutant on the adsorbed phase is discarded when the catalyst is irradiated, allowing the material to keep a certain level of performance on a next usage (***Fig 6. (b)(c)).*** With alternate phases without and then with UV irradiation (***Fig. 6.c***), the pollutant on the adsorbed phase decreases only when the system starts to be irradiated. If not, the adsorbed pollutant just accumulates gradually on the material, over repeated runs (***Fig. 6.a***).

Fig. 6.

A number of reasons could be applicable for explaining the catalysts efficiency gradual losses over successive treatment runs. Firstly, the location of the adsorbed pollutant molecules as compared to the position of the photocatalytic TiO_2-NPs centers within the composite catalyst. As discussed in section 2.1, TiO_2-NPs are preferentially located at the superficial macropores of the catalysts while typical adsorption of pollutant takes place within internal micropores where wider surface areas are developed. Additionally to irreversible adsorption of pollutant [17], their transfer limitations on the material (***Fig. 2.B***) could significantly reduce the probability of reaction with TiO_2 photogenerated reactive species. This could virtually participate to the accumulation of the pollutant on the catalyst over several treatment runs, despite the removal contribution of the photocatalytic degradation under UV light irradiation (***Fig 6. b.c***).

In the perspective of reaching higher global decontamination rate through several utilization, the fate of the pollutant accumulated on the catalyst should pay more attention. Strategies are to be addressed in order to enhance the efficiency of pollutant degradation once accumulated on the adsorbing catalyst. The surface chemistry, the fate of pollutant within the confined micropores and the photocatalytic specific contribution of AC component, are likely to play key roles on the overall decontamination capacity of AC-TiO_2 composite materials.

4. Conclusion

Adsorption-photodegradation synergy can be exploited with AC-TiO_2 composite materials for water depollution, towards biorefractories pollutants in particular. This paper aimed to provide a straightforward but realistic kinetic model to get insight interaction of both adsorption and photodegradation phenomena regarding phenol elimination. The straightforward preparation route of the composite catalysts used in this study enabled TiO_2-NPs to locate at the external porosity of the composite material, more accessible to UV irradiation. Owing to the

mathematical model set in this study, two basic parameters k_{ads} and α have been defined, respectively associated: (i) to global diffusion and the adsorption of the pollutant within the composite matrix, and (ii) to intrinsic photodegradation capacity of the catalyst. The consistency of the simulated kinetic breakthrough curves as compared to the experimental data under different conditions of experiment has been demonstrated. This suggests the feasibility of using a simple numerical tool in modelling adsorption/degradation coupled phenomena on AC-TiO_2. To the best of the author's knowledge, this novel modelling approach is used for the first time on AC-TiO_2 catalysts and in the future, could back up new more complex and theoretical modelling formalisms.

Acknoledgements

This research was supported by the "*Action Incitative AI-2014*" funding of CIRAD-France

List of symbols

C_o initial concentration of the pollutant in the solution (mg.L^{-1})
C_{cal}, C_{exp} calculated and experimental concentrations of the pollutant in the solution (mg.L^{-1})
C_{cat} concentration of the catalyst in the solution (g.L^{-1})
C_t concentration of the pollutant in the solution (mg.L^{-1})
CRIT optimization criteria in numerial modelling (-)
I_{UV} UV light intensity (W.m^{-2})
K distribution coefficient (-)
k_{ads} adsorption rate coefficient (s^{-1})
k_r photodegradation rate coefficient (s^{-1})
n_{exp} number of experiments (-)
q_e, q_f adsorption capacities of the catalyst at the equilibrium and at the end of the run (mg.g^{-1})
q_t adsorption capacity of the catalyst (mg.g^{-1})
N_f pollutant density flux onto the catalyst (mg.s^{-1}.g^{-1})
S surface of the reactor (m^2)
t time (s)
V volume of the reactor (m^3)
α photodegradation rate constant (m^2.J^{-1})

References

[1] M. Miguet, V. Goetz, G. Plantard, Y. Jaeger, Ind. Eng. Chem. Res. 54 (2015) 9813–9823.
[2] F. Salvador, N. Martin-Sanchez, R. Sanchez-Hernandez, M.J. Sanchez-Montero, C. Izquierdo, Microporous Mesoporous Mater. 202 (2015) 259–276.
[3] Z. Xing, J. Zhang, J. Cui, J. Yin, T. Zhao, J. Kuang, Z. Xiu, N. Wan, W. Zhou, Appl. Catal. B Environ. 225 (2018) 452–467.
[4] T.-T. Lim, P.-S. Yap, M. Srinivasan, A.G. Fane, Crit. Rev. Environ. Sci. Technol. 41 (2011) 1173–1230.
[5] J. Schneider, M. Matsuoka, M. Takeuchi, J. Zhang, Y. Horiuchi, M. Anpo, D.W. Bahnemann, Chem. Rev. 114 (2014) 9919–9986.
[6] C. Liu, Y. Li, P. Xu, M. Li, M. Zeng, Mater. Chem. Phys. 149–150 (2015) 69–76.
[7] Z. Sun, X. He, J. Du, W. Gong, Environ. Sci. Pollut. Res. 23 (2016) 21733–21740.
[8] F. Tian, Z. Wu, Q. Chen, Y. Yan, G. Cravotto, Z. Wu, Appl. Surf. Sci. 351 (2015) 104–112.
[9] C.T. Chekem, Y. Richardson, G. Plantard, J. Blin, V. Goetz, Waste Biomass Valorization (2016) 1–13.

[10] P.-S. Yap, T.-T. Lim, Water Res. 46 (2012) 3054–3064.
[11] S.X. Liu, C.L. Sun, S.R. Zhang, Bull. Environ. Contam. Toxicol. 73 (2004) 1017–1024.
[12] Y. Li, X. Li, J. Li, J. Yin, Water Res. 40 (2006) 1119–1126.
[13] L.F. Velasco, B. Tsyntsarski, B. Petrova, T. Budinova, N. Petrov, J.B. Parra, C.O. Ania, J. Hazard. Mater. 184 (2010) 843–848.
[14] X. Wang, Z. Hu, Y. Chen, G. Zhao, Y. Liu, Z. Wen, Appl. Surf. Sci. 255 (2009) 3953–3958.
[15] V. Goetz, T. Janin, G. Plantard, S. Brosillon, Int. J. Eng. Pract. Res. 2 (2013) 86–93.
[16] C.T. Chekem, Y. Richardson, M. Drobek, G. Plantard, J. Blin, V. Goetz, React. Kinet. Mech. Catal. (2017) 1–25.
[17] A. Gomis-Berenguer, L.F. Velasco, I. Velo-Gala, C.O. Ania, J. Colloid Interface Sci. 490 (2017) 879–901.
[18] C.S. Turchi, D.F. Ollis, J. Catal. 122 (1990) 178–192.
[19] M.F.F. Sze, G. McKay, Water Res. 46 (2012) 700–710.
[20] L.F. Velasco, C.O. Ania, Adsorption 17 (2011) 247–254.
[21] M. el M. Zekri, C. Colbeau-Justin, Chem. Eng. J. 225 (2013) 547–557.
[22] A.E. Cassano, O.M. Alfano, Catal. Today 58 (2000) 167–197.
[23] O.M. Alfano, D. Bahnemann, A.E. Cassano, R. Dillert, R. Goslich, Catal. Today 58 (2000) 199–230.
[24] V. Goetz, J.P. Cambon, D. Sacco, G. Plantard, Chem. Eng. Process. Process Intensif. 48 (2009) 532–537.
[25] D. Ollis, in: P. Pichat (Ed.), Photocatal. Water Purif., Wiley-VCH Verlag GmbH & Co. KGaA, 2013, pp. 311–333.
[26] A.T. Mohd Din, B.H. Hameed, A.L. Ahmad, J. Hazard. Mater. 161 (2009) 1522–1529.
[27] N. Roostaei, F.H. Tezel, J. Environ. Manage. 70 (2004) 157–164.

Liste of Figures

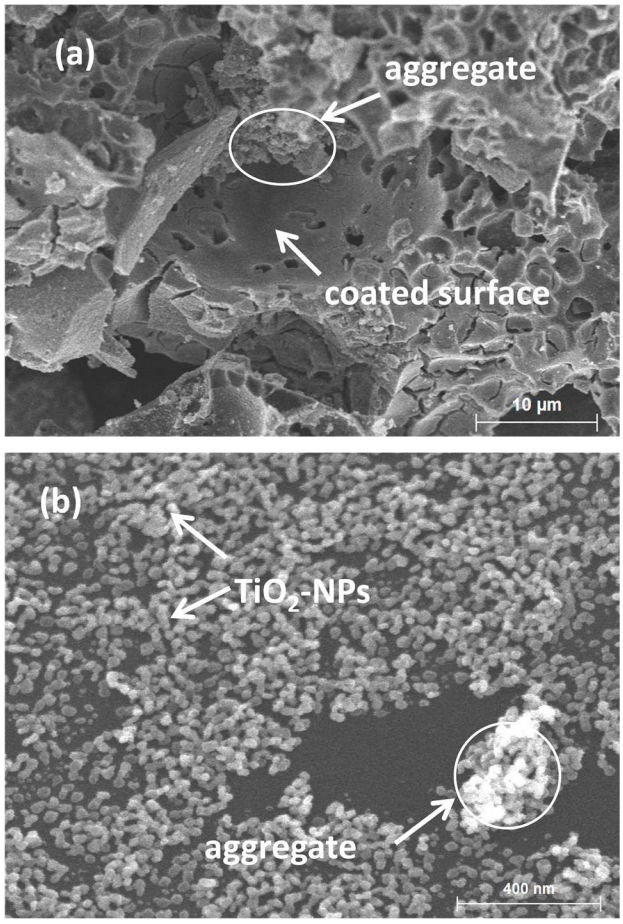

Fig. 1. FESEM images on the surface of *CAT25* sample (a) macropores and (b) TiO_2 nanoparticles

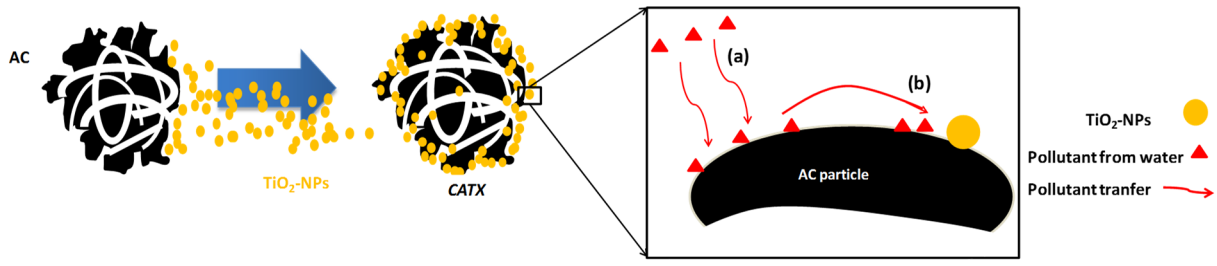

(A) (B)

Fig.2. Illustration scheme of (A) TiO_2-NPs fixation at the external porosity of AC support (B) pollutant transfer towards photocatalytic centers

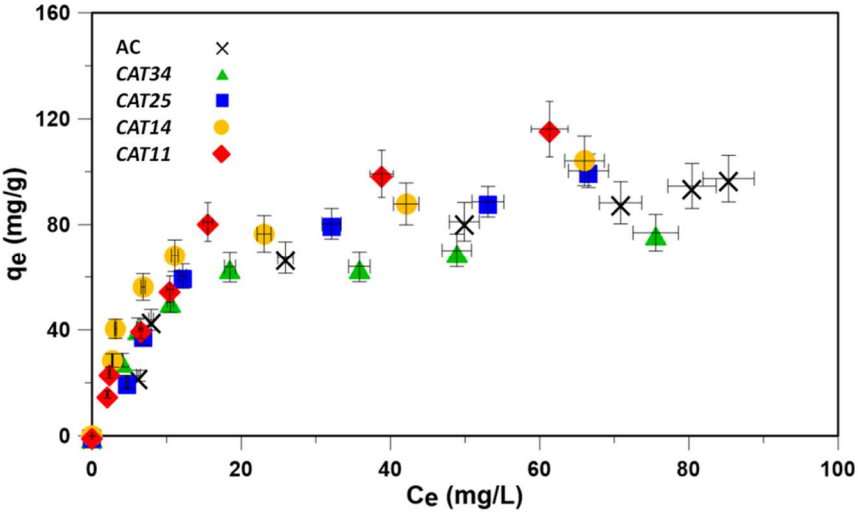

Fig. 3. Experimental phenol adsorption isotherms of uncoated AC and composite materials

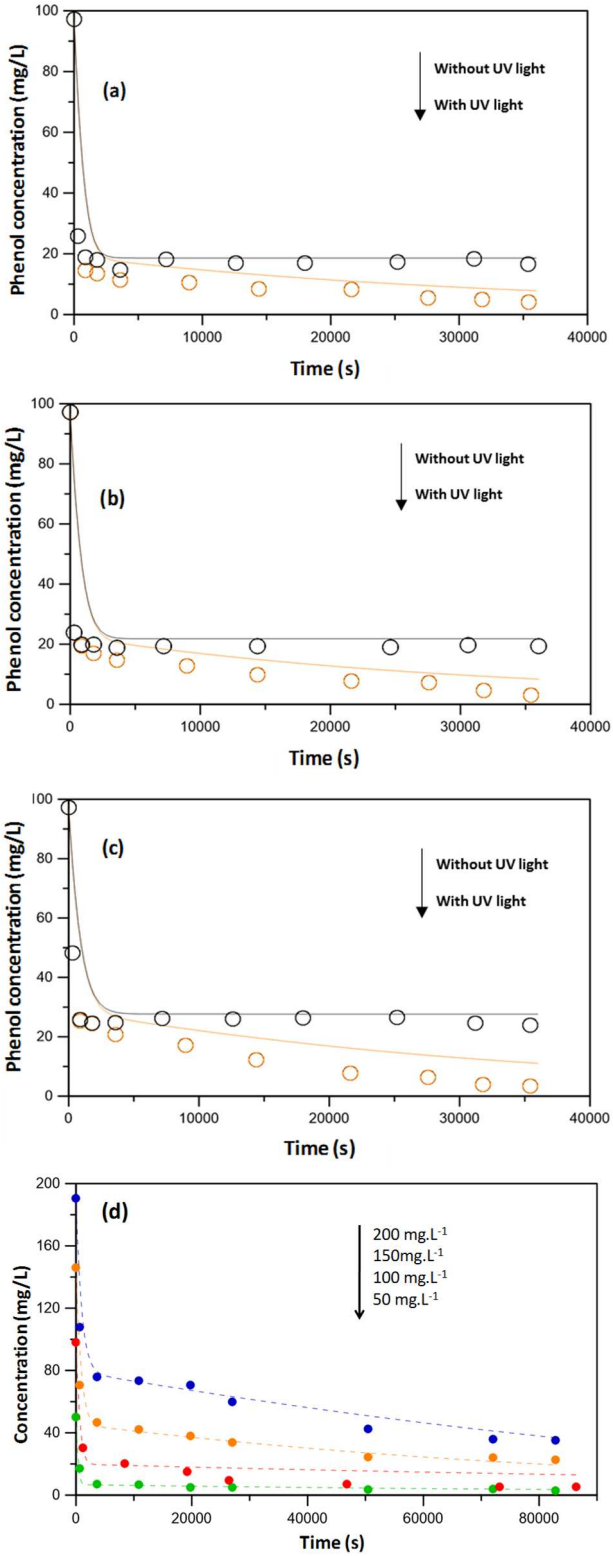

Fig.4. Experimental (points) and simulated (lines) kinetics of phenol disappearance in the polluted water using different catalysts **(a)** *CAT14* **(b)** *CAT25* **(c)** *CAT36* and **(d)** at different initial phenol concentrations with *CAT25*

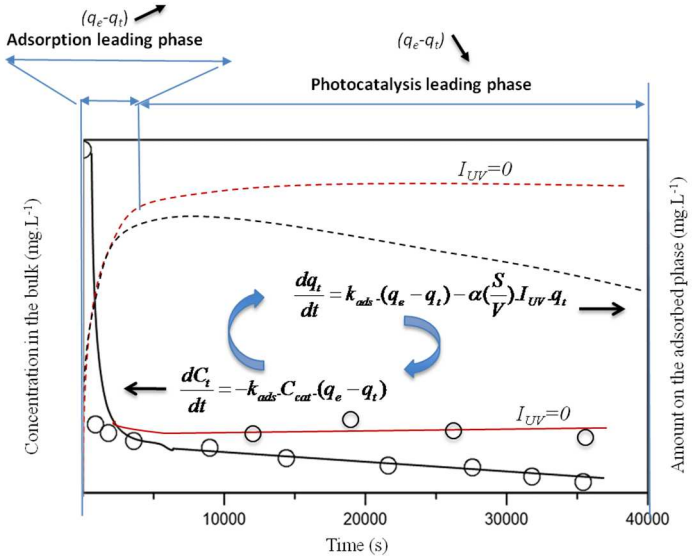

Fig.5. Representative scheme of adsorption/photodegradation interaction over the profile of pollutant on the bulk (continuous lines + experimental points) and adsorbed phases (dot lines)

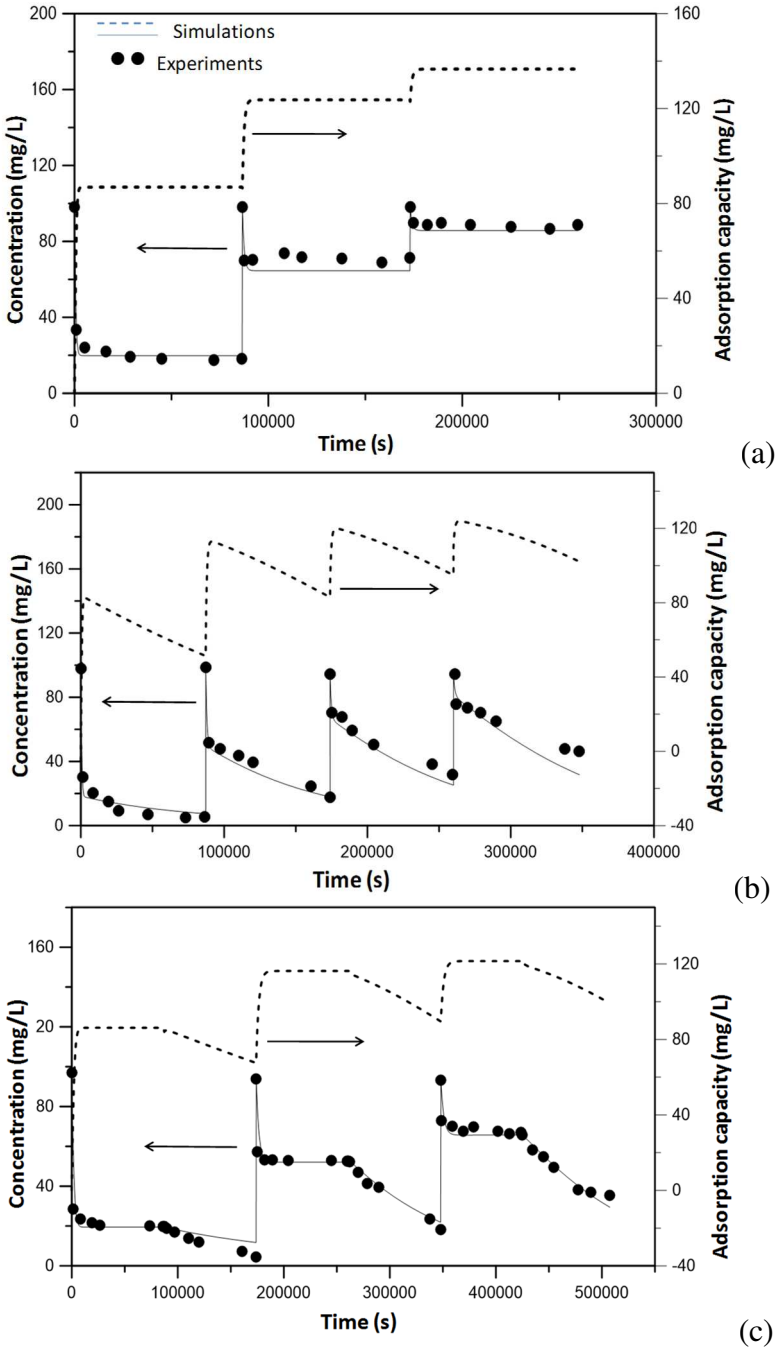

Fig. 6. Phenol concentration profile in the solution (Experimental (points) and simulation (continuous lines)), and on *CAT25* (simulated dot lines) using (a) without UV light (b) under UV light (c) alternate phase without and with UV light

List of Tables

Table 1. Textural and structural related parameters of AC and AC-TiO_2 catalysts.

Sample	TiO_2[a] (% Wt)	S_{BET} (m^2/g)	[1]V_{Total} (cm^3/g)	[2]V_{micro} (cm^3/g)	Langmuir model parameters $q_e = \frac{q_{max} \cdot K_L \cdot C_e}{1 + K_L \cdot C_e}$		
					K_L ($L.mg^{-1}$)	q_{max} ($mg.g^{-1}$)	R^2
AC	0	571	0.272	0.252	0.079	117.4	0,975
CAT 14	14	631	0.298	0.253	0.082	111.5	0.958
CAT 25	25	609	0.285	0.248	0.091	124.5	0.952
CAT 34	34	602	0.286	0.257	0.073	82.3	0.942

[a]anatase ; [1] total pore volume evaluated at $P/P_0 \approx 0.99$; [2] evaluated from DFT method applied to N_2 adsorption at -196 °C

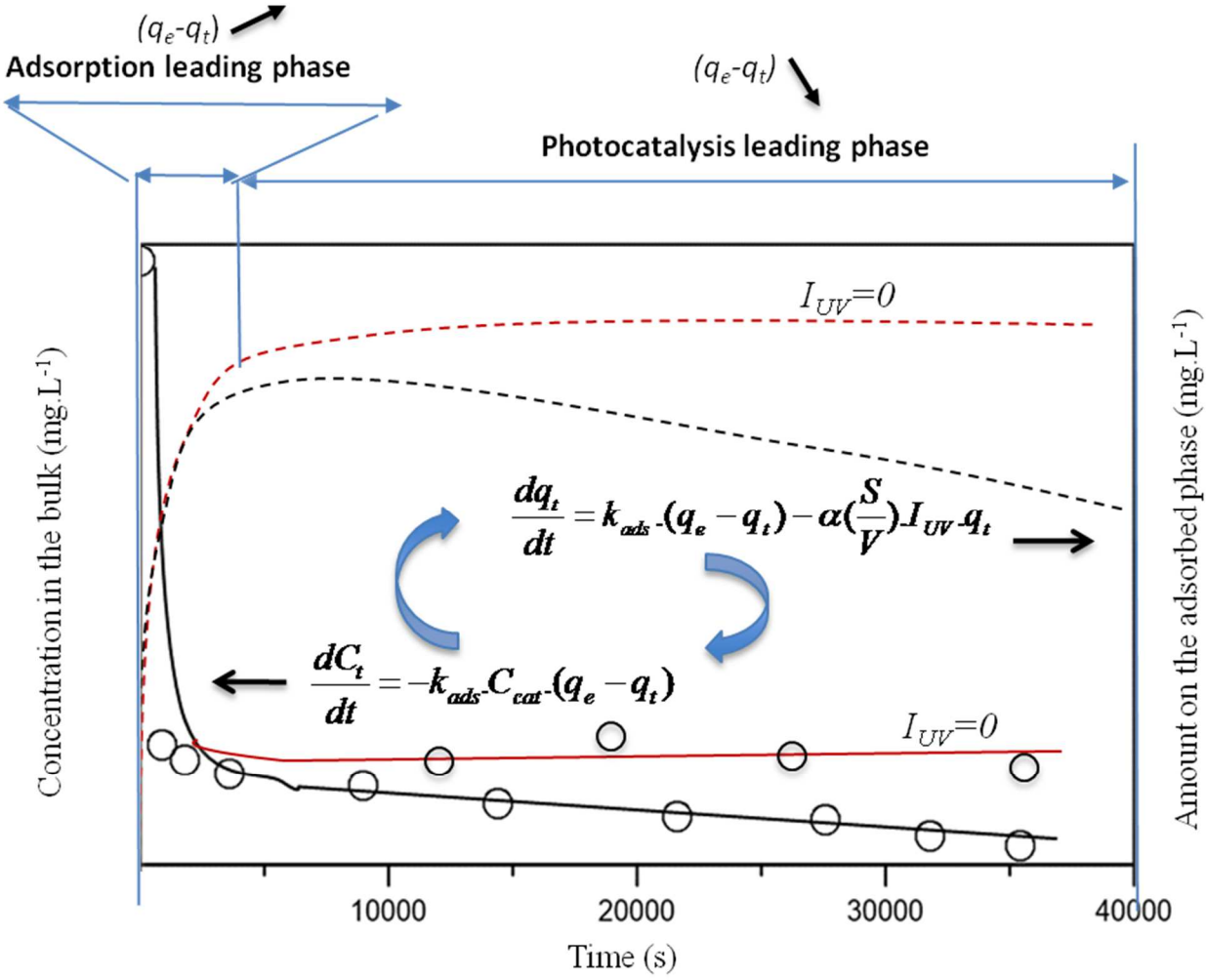
$(q_e\text{-}q_t)$
Adsorption leading phase
$(q_e\text{-}q_t)$
Photocatalysis leading phase
$I_{UV}=0$
$\frac{dq_t}{dt} = k_{ads}\text{-}(q_e - q_t) - \alpha(\frac{S}{V})I_{UV}\text{-}q_t$
$\frac{dC_t}{dt} = -k_{ads}\text{-}C_{cat}\text{-}(q_e - q_t)$
$I_{UV}=0$
Concentration in the bulk (mg.L^{-1})
Amount on the adsorbed phase (mg.L^{-1})
10000
20000
30000
40000
Time (s)